EPJ Web of Conferences **151**, 03006 (2017) DOI: 10.1051/epjconf/201715103006
LAM-16

Structure and Ionic Diffusion in Molten NaI, RbI, and NaI-RbI mixture

Shuta Tahara[1,2,*], *Koji* Ohara[2], *Hironori* Shimakura[3], and *Takanori* Fukami[1]

[1]Department of Physics and Earth Sciences, Faculty of Science, University of the Ryukyus, Okinawa 903-0213, Japan
[2]Research and Utilization Division, Japan Synchrotron Radiation Research Institute (JASRI, SPring-8), Hyogo 679-5198, Japan
[3]Niigata University of Pharmacy and Applied Life Sciences, Niigata 956-8603, Japan

Abstract. Static structure factors of molten NaI, RbI, and their mixture of $(RbI)_{0.3}(NaI)_{0.7}$ are measured up to high-Q region by using the high-energy X-ray diffraction technique. Moreover, molecular dynamics (MD) simulations are carried out, and the simulation results well reproduce the diffraction data. The partial structure factors, partial pair distribution functions, and ionic diffusion coefficients calculated by the MD simulations are reported in detail. The mixing effects of cations on the structure and ionic diffusion are also discussed.

1 Introduction

Both experimental and theoretical approaches are important to investigate the physical properties of the liquid materials including molten salts. For example, the structure of molten NaCl has been studied by using the neutron diffraction measurements with isotopic substitution technique by Edwards et al [1], and their partial structure factors and partial pair distribution functions have been well reproduced by the molecular dynamics (MD) simulation by Dixon and Sangster [2], and Ciccotti et al. [3]. The ionic transport properties have also been discussed on the basis of the simulation results.

NaI is one of the simple salts, however the experimental structure-data for the molten phase is rare. Specifically, McGreevy et al. have measured the dynamic structure factor $S(Q,\omega)$ by using the inelastic neutron scattering technique in 1984. They have reported the broadening of the quasi-elastic peak associated with diffusion together with an extended inelastic spectrum associated with corrective motion [4]. They have also estimated the total static structure factor $S(Q)$ for molten NaI up to approximately $Q = 2$ Å^{-1} from the analysis of $S(Q,\omega)$, and they pointed out that the simulation results in the low-Q region by Dixon and Sangster show the good agreement with the experimental $S(Q)$ [4]. Recently, Alcaraz et al. have also carried out the MD simulations with new models, and their simulation have well reproduced the experimental $S(Q)$ obtained by McGreevy et al. in the low-Q region [5,6]. Although McGreevy's experimental $S(Q)$ for molten NaI is very important and pioneering, an experimental $S(Q)$ up to relative high-Q is needed to investigate deeply the physical properties, and to confirm the validity of the theoretical model in a wide Q-range.

* Corresponding author: tahara@sci.u-ryukyu.ac.jp

In this paper, we report $S(Q)$ for molten NaI, RbI measured by high energy X-ray diffraction (HEXRD) technique up to Q = 15 Å^{-1}. Moreover, we carry out the MD simulation to compare with the experimental data with the simple model and parameters suggested by Ciccotti et al. [3], and the information on the partial structures and ionic transport properties are obtained. The $S(Q)$ for the mixture melt of $(RbI)_{0.3}(NaI)_{0.7}$ is also obtained by HEXRD experiment and MD simulation to investigate the mixture effects of different cation on the structure and ionic transport.

2 Methods

2.1 High-energy X-ray diffraction measurement

Each powder sample of NaI, RbI and their mixture of $(RbI)_{0.3}(NaI)_{0.7}$ sealed in a quartz tube under vacuum was once melted at 1023K, and then cooled to ambient temperature to form a bulk. The bulk samples were sealed in a fused silica capillary with 2.4 mm inner diameter and 0.25 mm wall thickness. The HEXRD experiments for molten states of these samples were carried out at 973K using a two-axis diffractometer installed at the BL04B2 beamline [7] at SPring-8. The incident X-ray beam from a Si(111) monochromator with the third harmonic reflection was 113.4 keV in energy and 0.1093 Å in wavelength. The measured X-ray diffraction data were corrected for polarization, absorption, and background contribution from the capillary and the instrument, and then the contribution of Compton scattering was also subtracted. The corrected data sets were normalized to give the Faber-Ziman [8] structure factor $S(Q)$.

2.2 Molecular dynamics simulation

MD simulations were carried out for molten NaI, RbI and $(RbI)_{0.3}(NaI)_{0.7}$ at the same temperature (973K) as the experiments. In this study, we used the Born-Mayer potential which is often used for simple alkali halide melts expressed as

$$\phi_{ij} = z_i z_j e^2/r + B_{ij}\exp(-\gamma_{ij} r) - C_{ij}/r^6 - D_{ij}/r^8. \quad (1)$$

The first term on the right-hand side is Coulomb interaction between ionic charges where z_{Na}, z_{Rb} and z_I were set as +1, +1 and -1, respectively. The second term is a repulsion between the ions arising from the overlap of the outer shell of electrons. The B_{ij} in the second term is expressed as $B_{ij} = \beta_{ij} b \exp[\gamma_{ij}(\sigma_i+\sigma_j)]$, where σ denotes ionic radius. The third and forth terms are van der Waals interactions. The potential parameters for pure NaI and RbI were taken from the earlier work [3]. For molten $(RbI)_{0.3}(NaI)_{0.7}$, the parameters were estimated from those for pure melts as listed in Table 1.

	B_{ij}	C_{ij}	D_{ij}
Na-Na	7.862	0.073	0.035
Na-Rb	37.578	0.433	0.351
Na-I	49.549	1.128	1.303
Rb-Rb	225.488	2.575	3.554
Rb-I	282.196	6.705	13.094
I-I	317.685	17.459	48.980

The potential parameters for the molten mixture were estimated as follows. For the repulsion interaction term, the Pauling factors were $\beta_{++} = 1.25$, $\beta_{+-} = 1$ and $\beta_{--} = 0.75$, and the strength parameter b was the same value of 0.211 eV for all interactions as written in Ref. 3. The γ_{ij} for the mixture was estimated from $\gamma_{ij} = 1 / (\varrho_i + \varrho_j)$, which is the same manner in Ref. 9. The C_{II} and D_{II} for the mixture were linearly interpolated between pure NaI and RbI. The C_{ij} and D_{ij} for unlike-ion pairs were estimated by geometric mean of those for like-ion interactions, which is similar manner to the Lorentz-Berthelot combining rules for the Lennard-Jones potential as written in Refs. 10 and 11. Since any experimental number density of the NaI-RbI mixture has not been reported, we attempted to estimate the number density of the mixture melt with several methods; (a) linear interpolation of the number densities of the pure melts (0.0200 [1/Å^3]) where the number densities of pure molten NaI and RbI are 0.0217 Å^{-3} and 0.0161 Å^{-3}, respectively [12], (b) linear interpolation of the molar volume of the pure melts (0.0196 [1/Å^3]), (c) the inversion from experimental $S(Q)$ to $g(r)$ (0.0200±0.0005[1/Å^3]). In this case, the number density estimated by the method (c) is almost the same as that estimated by the method (a). Therefore, we used 0.0200 Å^{-3} in this simulation. The simulation step was set as 5 fs and 1000 ionic particles (N_{Na} : 350, N_{Rb} : 150, N_I : 500) were placed in the simulation cell. The quantities of interest were obtained by taking the average over 20000 time steps which corresponds to 100 ps.

3 Results and discussion

3.1 Static structure

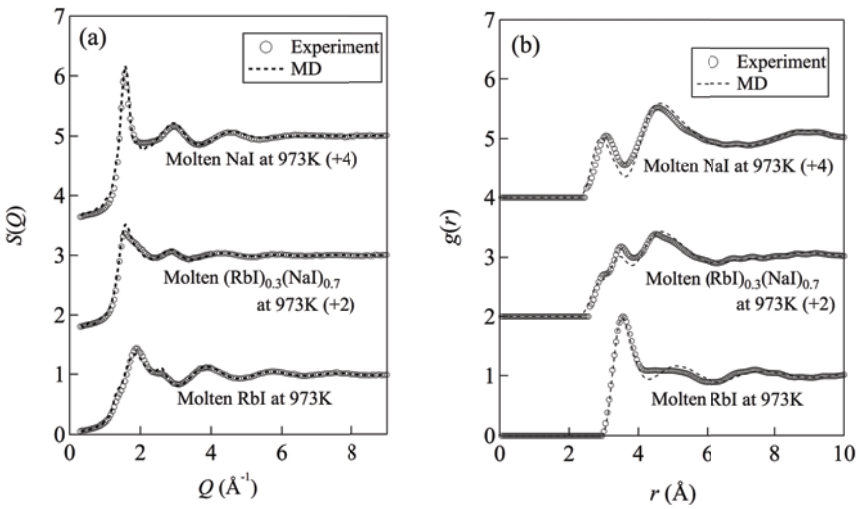

Fig. 1. (a) Faber-Ziman structure factors and (b) pair distribution functions for molten NaI, RbI and their mixture of $(RbI)_{0.3}(NaI)_{0.7}$ at 973K. The experimental data and MD simulation results are denoted by open circles and dashed curves, respectively.

The Faber-Ziman $S(Q)$ for molten NaI, RbI and $(RbI)_{0.3}(NaI)_{0.7}$ obtained by HEXRD are exhibited in Fig. 1(a). Although the $S(Q)$ were measured up to 15 Å^{-1}, the $S(Q)$ are basically unity for $Q > 9$ Å^{-1}. The first, second and third peaks for molten NaI are observed at around $Q = 1.5$, 2.9 and 4.5 Å^{-1}, respectively. The first peak of molten NaI was observed as a small pre-peak in $S(Q)$ estimated by the inelastic neutron scattering [4]. The differences in peak

heights between HEXRD and neutron scattering are due to the difference in weighting factor of partial correlations between X-ray and neutron scatterings. The first peak in $S(Q)$ for molten RbI is observed at around Q = 1.9 Å^{-1} with a hump (Q = 1.4 Å^{-1}) and a shoulder (Q = 2.6 Å^{-1}). The second and third peaks are observed at around Q = 3.9 and 5.8 Å^{-1}, respectively. While the peak positions in $S(Q)$ for $(RbI)_{0.3}(NaI)_{0.7}$ are similar to those for pure NaI because of the high concentration of NaI, the peak widths of the first and third peaks are broader than those for pure molten NaI. These peak broadenings would be caused by the differences in peak positions between pure NaI and RbI. For example, the shoulder-like feature of the first peak for $(RbI)_{0.3}(NaI)_{0.7}$ at around Q = 2 Å^{-1} corresponds to the first peak position of pure RbI. The MD results well reproduce the experimental data as shown in Fig. 1(a), which suggests that the potentials and parameters used in this study are reasonable.

Figure 1(b) shows pair distribution functions $g(r)$ for molten NaI, RbI, and $(RbI)_{0.3}(NaI)_{0.7}$ at 973K together with the results of MD simulations. These $g(r)$ were obtained by Fourier transform to the $S(Q)$. The first and second peaks in $g(r)$ for molten NaI are observed at around r = 3.1 and 4.6 Å, respectively. For RbI, the intense first peak and the vague second peak are observed at around r = 3.6 and 5 Å, respectively. We refer to the positions of the first and second peaks in $g(r)$ as r_1 and r_2 in the following discussions, respectively. Since r_1 corresponds to the first neighboring distance of unlike-ion pairs [3], the difference between r_1^{NaI} and r_1^{RbI} would reflect the difference in ionic radii between Na and Rb. In molten $(RbI)_{0.3}(NaI)_{0.7}$, two peaks are observed at around r = 3.0 and 3.5 Å which correspond to the first neighboring distances of Na-I (r_1^{NaI}) and Rb-I (r_1^{RbI}) correlations, respectively. The peak for molten $(RbI)_{0.3}(NaI)_{0.7}$ at around r = 4.5 Å corresponds to r_2^{NaI} which is mainly contributed by the first neighboring distance of Na-Na and I-I pairs [3]. These results suggest that the effects of mixing of two pure melts on the first neighboring distance of each correlation are small. The MD results are also shown in Fig. 1(b) and well reproduce the experimental $g(r)$.

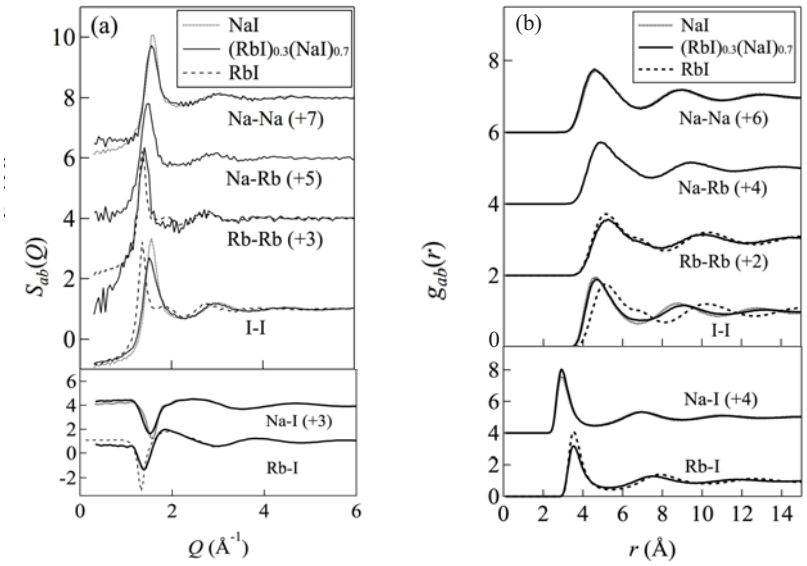

Fig. 2. (a) Faber-Ziman partial structure factors and (b) partial pair distribution functions for molten NaI (dotted curve), RbI (dashed curve) and their mixture of $(RbI)_{0.3}(NaI)_{0.7}$ (solid line) at 973K.

The Faber-Ziman partial structure factors $S_{ab}(Q)$ obtained by the MD simulations for molten NaI, RbI and $(RbI)_{0.3}(NaI)_{0.7}$ are shown in Fig. 2(a). Overall features of $S_{NaRb}(Q)$ is similar to $S_{NaNa}(Q)$ and $S_{RbRb}(Q)$, because Na and Rb ions are largely affected by the repulsion force between their positive charges. The first peak position of $S_{II}(Q)$ for the mixture is observed at between those for the pure melts, suggesting that the dense random packing of I ions are easily affected by the variety of density.

Figure 2(b) shows the partial pair distribution functions $g_{ab}(r)$ obtained by MD simulations for molten NaI, RbI and $(RbI)_{0.3}(NaI)_{0.7}$. The $g_{NaNa}(r)$ for pure NaI and the mixture coincide with each other, demonstrating that Na-Na correlation is not affected by Rb ions. On the other hand, Rb-Rb correlations show a slight difference between pure RbI and the mixture. For example, the shoulder observed at around r = 6.8 Å in $g_{RbRb}(r)$ for pure RbI becomes vague in the mixture. A slight shift of the second peak in $g_{RbRb}(r)$ from r = 10.1 Å for pure melt to 9.8 Å for the mixture is also observed, which would be affected by difference in the density between the pure RbI and the mixture. Each peak position for Na-Rb correlation for the mixture corresponds to the average of the peak positions for $g_{NaNa}(r)$ and $g_{RbRb}(r)$, for example the first peaks in $g_{NaNa}(r)$, $g_{NaRb}(r)$ and $g_{RbRb}(r)$ are observed at r = 4.5, 4.8 and 5.1 Å, respectively. The $g_{II}(r)$ is the most affected by the difference in densities among these melts. The first neighboring distances of unlike-chage pairs Na-I and Rb-I are 3 and 3.5 Å, respectively, which are also affected by the difference in ionic radii of Na and Rb.

3.2 Ionic transport

The diffusion coefficients D_α (10^{-5} cm^2/s) (α = Na, Rb, I) and ionic conductivities σ calculated by the MD simulations for molten NaI, RbI and their mixture at 973 K are summarized in Table 2 with experimental literature values for pure NaI [12] and RbI [13]. Ionic conductivities of the MD simulations are estimated by using Nernst-Einstein equation expressed as

$$\sigma = e^2 \left(\Sigma \rho_\alpha D_\alpha\right) / k_B T$$

where e, k_B, and ρ_α denote elemental charge, Boltzmann constant, and partial number density, respectively. The experimental ionic conductivities and diffusion coefficients are reasonably reproduced by MD simulations. Since ionic conductivities and diffusion coefficients for the mixture have not been measured, the MD results for the mixture cannot be compared to experimental data at this time. Although we used the rigid ion model in this study, if we consider a polarizable ion model, the cation diffusion would become large. However, polarization effects on NaI, RbI, and their mixture would be weak compared to silver (or cupper) halides [13-20] and zinc halides [21,22].

Ciccotti et al. have reported that D_{Na} and D_I for pure NaI at 1081K are 9.4 × 10^{-5} and 6.8 × 10^{-5} cm^2/s, respectively [3]. Therefore, the D_{Na} and D_I for pure NaI at 973K in this study are decreased by approximately 26% and 22% compared to the results at 1081K because of the decrease of the temperature. The D_{Rb} and D_I for pure RbI at 973K are also decreased by approximately 44% and 31% in comparison with the D_{Rb} (4.3 × 10^{-5} cm^2/s) and D_I (3.5 × 10^{-5} cm^2/s) at 1081K, respectively [3]. The D_{Rb} for the mixture is 2.25 times to that for pure RbI, while D_{Na} for the mixture is decreased by approximately 19% compared to that for pure NaI at the same temperature of 973K.

From the comparisons between the pure melts and the mixture melt, Na ions in the mixture diffuse slower than Na ions in pure NaI, while Rb ions in the mixture diffuse faster than Rb ions in pure RbI. These results suggest that the diffusion of Na ions would be disturbed by slow Rb ions, and the diffusion of Rb ions would be promoted by fast Na ions because of the repulsive interaction between Na and Rb ions, and resultant D_{Na} and D_I for

the mixture would show similar values each other. Since the D_I for the mixture is twice as large as that for pure RbI, diffusion of I ions might also be affected by the attractive interaction from fast Na ions. Although the mixture effects of cations on Na-Na and Rb-Rb partial structures are very small, the effects on the ionic diffusion are large.

Table 2. Diffusion coefficients D_α (10^{-5}cm^2/s), for Na, Rb and I ions in molten NaI, RbI and $(RbI)_{0.3}(NaI)_{0.7}$ at 973K. Parentheses denote experimental literature values.

	NaI	RbI	$(RbI)_{0.3}(NaI)_{0.7}$
D_{Na} (10^{-5}cm^2/s)	7.0 (7.35 [12])		5.7
D_{Rb} (10^{-5}cm^2/s)		2.4	5.4
D_I (10^{-5}cm^2/s)	5.3 (4.05 [12])	2.4	4.5
σ (S/cm)	2.55 (2.38 [12])	0.74 (0.84 [13])	1.93

4 Summary

We have measured the $S(Q)$ for molten NaI, RbI, and their mixture of $(RbI)_{0.3}(NaI)_{0.7}$ up to Q = 15 Å^{-1}. These $S(Q)$ have been well reproduced by the MD simulations with the simple Born-Mayer potentials and parameters reported by the literature [3]. The $S_{ab}(Q)$ and $g_{ab}(r)$ have been obtained by the MD simulations. The structural feature for Na-Rb correlation in the mixture is similar to those for Na-Na and Rb-Rb correlations. The $S_{II}(Q)$ and $g_{II}(r)$ are largely depend on the materials, suggesting that the dense random packing of I ions are easily affected by the variety of density, which is the mixing effect of the cations on the structure. The D_α for the pure and mixture melts have also been calculated by the MD simulations. The D_α for the pure melts at 973 K in this study shows the decrease compared to that at 1081 K reported by the earlier work [3]. The D_α of all the ionic species in the mixture is different from that in the pure melts, which is the mixing effect of the cations on the ionic diffusions. While the mixture effects of cations on Na-Na and Rb-Rb partial structures are very small, the effects on the ionic diffusion are large.

The synchrotron radiation experiments were performed at the BL04B2 at SPring-8 with the approval of the Japan Synchrotron Radiation Research Institute (JASRI, proposal 2011B1531).

References

1. F. G. Edwards, J. E. Enderby, R. A. Howe, D. I. Page, J. Phys. C: Solid State Phys. **8**, 3483 (1975)
2. M. Dixon, M. J. L. Sangster, J. Phys. C: Solid State Phys. **9**, 909 (1976)
3. G. Ciccotti, G. Jacucci, I. R. McDonald, Phys. Rev. A **13**, 426 (1976)
4. R. L. McGreevy, E. W. J. Mitchell, F. M. A. Margaca, J. Phys. C: Solid State Phys. **17**, 775 (1984)
5. O. Alcaraz, J. Trullàs, J. Mol. Liq. **136**, 227 (2007)
6. O. Alcaraz, V. Bitrián, J. Trullàs, J. Chem. Phys. **127,** 154508 (2007)
7. S. Kohara, M. Itou, K. Suzuya, Y. Inamura, Y. Sakurai, Y. Ohishi, M. Takata, J. Phys.: Condens. Matter **19**, 506101 (2007)
8. T. E. Faber, J. M. Ziman, Phil. Mag. **11**, 153 (1965)

9. R. Takagi, F. Hutchinson, P. Madden, A. K. Adya, M. Gaune-Escard, J. Phys.: Condens. Matter **11**, 645 (1999)
10. H. A. Lorentz, Ann. Phys. **12**, 127 (1881)
11. D. C. R. Berthelot, Hebd. Seanc. Acad. Sci. **126**, 1703 (1898)
12. G. J. Janz, *Molten salts handbook* (Academic Press, New York, 1967)
13. S. Tahara, S. Ohno, T. Okada, Y. Kawakita, S. Takeda, EPJ Web Conf. **15**, 02005 (2011)
14. J. Trullàs, O. Alcaraz, L. E. González, M. Silbert, J. Phys. Chem. B **107**, 282 (2003)
15. V. Bitrián, J. Trullàs, J. Phys. Chem. B **110**, 7490 (2006)
16. V. Bitrián, J. Trullàs, M. Silbert, T. Enosaki, Y. Kawakita, S. Takeda, J. Chem. Phys. **125**, 184510 (2006)
17. V. Bitrián, J. Trullàs, J. Phys. Chem. B **112**, 1718 (2008)
18. V. Bitrián, O. Alcaraz, J. Trullàs, J. Chem. Phys. **134**, 044501 (2011)
19. S. Tahara, T. Fukami, Journal of the Physical Society of Japan **84**, 024602 (2015)
20. S. Tahara, Y. Kawakita, H. Shimakura, K. Ohara, T. Fukami, S. Takeda, J. Chem. Phys. **143**, 044509 (2015)
21. M. Wilson and P. A. Madden, Phys. Rev. Lett. **72**, 3033 (1994)
22. M. Wilson and P. A. Madden, Phys. Rev. Lett. **80**, 532 (1998)